Research article

Snhg14/miR-181a-5p axis-mediated "M1" macrophages aggravate LPS-induced myocardial cell injury

Chenglong Bi [a], Dejin Wang [a], Bin Hao [b], Tianxiao Yang [a],[*]

[a] *Department of Cardiology, Shandong University Zibo Central Hospital, Zibo, 255000, Shandong, China*
[b] *Cardiovascular Surgery, Shandong University Zibo Central Hospital, Zibo, 255000, China*

ARTICLE INFO

ABSTRACT

An increasing number of studies have suggested that macrophages participate in sepsis-induced myocardial injury. Our study highlights the function and mechanism of the lncRNA Snhg14 in "M1" polarized macrophage-mediated myocardial cell damage. Lipopolysaccharide (LPS) was used to treat H9c2 cells to construct an *in vitro* myocardial injury model. M1 and M2 polarization of RAW264.7 cells were induced and the exosomes were obtained from the supernatant through ultracentrifugation. Moreover, cecal ligation and puncture (CLP) surgery was implemented to establish a mouse sepsis-induced myocardial injury model, and Snhg14 was knocked down with sh-Snhg14. The results showed that the conditioned medium (CM) and the exosomes (Exo) of M1 macrophages substantially augmented LPS-induced apoptosis and oxidative stress in myocardial cells. Notably, M1-CM and M1-Exo contributed to nearly 50 % of myocardial cell viability decline. Snhg14 was highly expressed in M1 macrophages and exosomes derived from M1-MΦ (M1-Exo). Snhg14 overexpression aggravated myocardial cell damage and increased 10 to 50 times expression of proinflammatory cytokines in MΦ. Snhg14 knockdown reversed M1-Exo-mediated myocardial cell damage and inhibited the production of proinflammatory cytokines (50 %–75 % decline) of MΦ. Moreover, Snhg14 targeted and inhibited miR-181a-5p expression. miR-181a-5p upregulation partly reversed Snhg4 overexpression-mediated myocardial cell damage and MΦ activation. *In vivo*, sh-Snhg14 dramatically ameliorated cardiac damage in septic mice by enhancing miR-181a-5p and inhibiting the HMGB1/NF-κB pathway. In conclusion, "M1" macrophage-derived exosomal Snhg14 aggravates myocardial cell damage by modulating the miR-181a-5p/HMGB1/NF-κB pathway.

1. Introduction

Sepsis is a systemic inflammatory syndrome caused by the invasion of pathogenic microorganisms such as bacteria into the body. It is clinically a leading contributor to the death of critical patients [1]. Sepsis-induced myocardial injury is the most prevalent complication of sepsis. Approximately 40 % of sepsis patients will develop myocardial damage, and sepsis-induced myocardial injury contributes to a death rate of 70 % [2]. Although sepsis-induced myocardial injury seriously threatens the life and health of people, there are no efficacious treatment options that can reverse myocardial dysfunction resulting from sepsis [3]. Thus, a better

---

* Corresponding author. Department of Cardiology, Shandong University Zibo Central Hospital, No. 10, South Shanghai Road, Zibo, 255000, China.
E-mail address: tianxiaoy1000@163.com (T. Yang).

understanding of the pathogenesis of sepsis-induced myocardial injury, which is highly important for preventing and treating this disease, is urgently needed.

Macrophages are phagocytes distributed in nearly all tissues of the body. The transformation of their M1/M2 polarization phenotypes is pivotal for efficaciously repressing inflammation after sepsis and inverting excessive cardiac function injury [4]. In recent years, an increasing number of studies have shown that macrophages participate in sepsis-induced myocardial injury [5–7]. Long noncoding RNAs (lncRNAs), a class of noncoding RNAs over 200 nucleotides in length, play a significant role in the occurrence and progression of sepsis [8]. For example, the lncRNA metastasis-associated lung adenocarcinoma transcript 1 (MALAT1) has been shown to be relevant to sepsis. MALAT1 is highly expressed in septic mice. MALAT1 downregulates microRNA-23a to increase mast cell-expressed membrane protein 1 (MCEMP1) expression to exacerbate inflammatory responses in mice with sepsis [9]. Small nucleolar host gene 14 (SNHG14) is another lncRNA. Knocking down SNHG14 repressed lipopolysaccharide (LPS)-induced PC-12 cell inflammation and apoptosis [10]. Moreover, SNHG14 plays a vital role in acute lung injury (ALI). The knockdown of SNHG14 with LPS induced the apoptosis and inflammation of lung epithelial cells by restoring the expression of miR-124-3p [11].

MicroRNAs (miRNAs), single-stranded noncoding RNAs approximately 20–24 nt in length, play a role in gene transcription and widely participate in the pathophysiological process of sepsis [12–14]. microRNA-181a-5p (miR-181a-5p), a member of the miRNA family, is involved in myocardial cell damage under pathological stimulation. For example, miR-181a-5p attenuates the apoptosis of myocardial cells treated with high glucose [15]. miR-181a-5p also participates in the pathogenesis of sepsis. Studies have revealed that in the context of sepsis, miR-181a-5p inhibition upregulates sirtuin-1 (SIRT1) to dampen the profiles of inflammatory cytokines and NF-κB signalling pathway activation, hence mitigating inflammatory responses in macrophages treated with LPS [16].

High Mobility Group Box 1 (HMGB1) is a nuclear protein in charge of DNA damage repair and the maintenance of genome stability [17]. Under pathological conditions of cellular stress or tissue injury, HMGB1 is translocated from the nucleus of injured cells to the cytoplasm and finally released into the extracellular environment [18]. HMGB1 acts a damage-associated molecular pattern (DAMP) molecule by binding to receptors such as the toll-like receptors (eg. TLR2, TLR4, TLR9) and receptor for advanced glycation end products (RAGE), thus leading to the activation of NF-κB pathway and enhancing the production of pro-inflammatory mediators [19, 20]. Elevated levels of circulating HMGB1 have been associated with the severity of sepsis and poor clinical outcomes [21]. HMGB1 plays a significant role in sepsis-associated myocardial injury by mediating inflammatory response and immune activation [22]. Additionally, HMGB1 can induce enhancement of paracellular gap formation and diminution of transendothelial cell electrical resistance (TER), leading to increased vascular permeability and impaired vascular tone regulation [23]. Due to its pivotal role in the inflammatory response and immune activation in sepsis, HMGB1 has emerged as a potential therapeutic target for the treatment of septic conditions.

Here, we revealed that M1 macrophages and their exosomes dramatically increased LPS-induced myocardial cell damage. Snhg14 was significantly elevated in M1-polarized macrophages and their exosomes. Snhg14 knockdown or miR-181a-5p overexpression weakened the ability of M1 macrophages to promote myocardial cell damage induced by LPS. Thus, we speculated that M1 macrophage-derived exosomal Snhg14 plays an essential role in myocardial cell damage. Our findings may provide new options for treating sepsis-induced myocardial injury.

2. Materials and methods

2.1. Cell culture and treatment

H9c2 and RAW264.7 cells, ordered from the American Type Culture Collection (ATCC, Rockville, MD, USA), were cultured in Dulbecco's modified Eagle's medium (DMEM) (Thermo Fisher Scientific, Waltham, MA, USA) supplemented with 10 % fetal bovine serum (FBS) (Sigma−Aldrich, Germany) and 100 U/mL/100 U/mL penicillin/streptomycin (Gibco, USA). The cells were incubated with 95 % humidity and 5 % CO_2 at 37 °C.

RAW264.7 cells were incubated with 150 nM phorbol 12-myristate 13-acetate (PMA) (Calbiochem, USA) for 24 h and then in DMEM for 24 h, after which they finally differentiated into M0 macrophages. Next, the cells were incubated with 20 ng/mL interferon-γ (IFN-γ) (R&D Systems, USA) plus 100 ng/mL lipopolysaccharide (LPS) (Sigma−Aldrich, Germany) for 48 h and polarized into M1 macrophages. Moreover, M0 macrophages were incubated with 20 ng/mL interleukin-4 (IL-4) (R&D Systems, USA) plus 20 ng/mL interleukin-13 (IL-13) (R&D Systems, USA) for 48 h and polarized into M2 macrophages [24].

LPS (5 μg/mL) was administered to H9c2 cells for 24 h to establish an *in vitro* myocardial damage model [25]. The conditioned medium and exosomes of the macrophages were used to treat the LPS (5 μg/mL)-induced myocardial cells for 24 h.

2.2. Cell transfection

GenePharma Co., Ltd. (Shanghai, China) provided Snhg14 overexpression plasmids, sh-Snhg14, miR-181a-5p mimics (50 nM), the miR-181a-5p inhibitor (100 nM) and corresponding negative controls (vector, sh-NC, miR-NC, and miR-in). The corresponding oligonucleotides were transfected into macrophages and myocardial cells via the Lipofectamine 2000 reagent (Invitrogen). Reverse transcription−polymerase chain reaction (RT−PCR) was used to determine the efficiency of transfection. Twenty-four hours after transfection, the cells were harvested for the following tests.

2.3. Separation and identification of exosomes

Ultracentrifugation was employed to isolate the exosomes referring to a previous study [26] with minor modifications. The supernatant of the macrophages was centrifuged at $500 \times g$ for 10 min to remove sediments and then centrifuged at $2000 \times g$ for 10 min to clear the cell debris. The supernatant was centrifuged at $10,000 \times g$ (30 min) to dislodge large-size shedding blisters. After that, the supernatant was harvested via a 0.22-μm filter, was centrifuged at $100000 \times g$ in an ultracentrifugation tube for 4 h. The harvested sediments were exosomes.

The size of isolated vesicles was measured through dynamic light scattering (DLS) technique using a ZetasizerNano ZS90 analysis system (Malvern, UK). We observed the morphology of the exosomes via transmission electron microscopy. The collected exosomes (50 μL) were dripped on 200-mesh copper mesh and incubated at room temperature (RT) for 5 min. Later, 1 % phosphotungstic acid was used to stain the exosomes for 1 min. The samples were washed in distilled water twice. Following drying, the copper mesh was observed via a TEM-1400 plus at 80 kV. Western blot analysis confirmed the profiles of exosome marker proteins (CD63, CD81, and CD9).

2.4. Cell Counting Kit-8 (CCK8)

After treatment, LPS-induced myocardial cells were inoculated into 6-well plates. Following 24 h of culture, 10 μl of CCK8 solution (Biosharp, HeFei, China) was added to each well. The culture dish was cultured in an incubator for 3 h. As instructed by the manufacturer, a microplate reader (Tecan Group Ltd., Switzerland) was used to measure the optical density at 450 nm to evaluate myocardial cell viability.

2.5. Terminal dUTP nick-end labelling (TUNEL)

After treatment, the myocardial cells were harvested, washed with PBS three times, and fixed with 4 % paraformaldehyde at RT for 20 min. The *In Situ* Cell Death Detection Kit and Fluorescein (Roche Diagnostics) were used for TUNEL staining according to the manufacturer's instructions. DAPI (0.1 μg/ml) was used to redye the nuclei for 5 min in darkness at RT. A fluorescence microscope (Olympus Corporation) was used to observe TUNEL-positive cells.

2.6. Detection of reactive oxygen species (ROS) levels

The ROS levels in the myocardial cells were verified via a DCFDA/H2DCFDA-Cellular ROS Assay Kit (ab113581; Abcam). The treated myocardial cells were inoculated into 6-well plates at a density of 3×10^5/well. After 24 h of culture, the cells were washed with PBS and stained with 20 μM 2′,7′-dichlorofluorescin diacetate (DCFDA) solution for 45 min at 37 °C. The cells were subsequently rinsed with $1 \times$ Buffer three times. A fluorescence microscope (BX53, Olympus, Japan) was used to examine and observe the fluorescence signal.

2.7. Detection of superoxide dismutase (SOD), malondialdehyde (MDA), caspase3, and caspase9 levels

As instructed by the manufacturer, commercial kits, including SOD (Cat.no. BC0170, Solarbio, Beijing, China), MDA (Cat.no. BC0025, Solarbio, Beijing, China), and Caspase3 (Cat.no. C1116, Beyotime, Shanghai, China) and Caspase9 (Cat.no. C1158, Beyotime, Shanghai, China) were used to determine the content or activity of SOD, MDA, Caspase3 and Caspase9 in H9c2 cells and myocardial tissues.

2.8. Enzyme-linked immunosorbent assay (ELISA)

In accordance with the manufacturer's instructions, ELISA kits (Boster Biological Technology, Wuhan, China) were used to measure the levels of tumor necrosis factor α (TNF-α), interleukin 1β (IL-1β), interleukin 6 (IL-6), and interleukin 10 (IL-10) in macrophages, the supernatant of myocardial cells, and myocardial tissues.

2.9. Western blot

Radioimmunoprecipitation assay (RIPA) lysis buffer was used to separate the total protein from myocardial cells, macrophages and their exosomes, and myocardial tissues. A bicinchoninic acid (BCA) kit (Beyotime Biotechnology) was used to determine the protein concentration. Protein samples (30 μg) were separated via 12 % sodium dodecyl sulfate–polyacrylamide gel electrophoresis (SDS–PAGE) and transferred onto polyvinylidene difluoride (PVDF) membranes (Millipore, MA, USA). After being blocked with 5 % skim milk for an hour, the membranes were incubated with primary antibodies overnight at 4 °C and then with a horseradish peroxidase (HRP)-labelled secondary antibody (1:2000, ab6728) for an hour at RT. Finally, an enhanced chemiluminescence kit (ECL, Millipore, Bedford, MA, USA) was used to observe the protein bands. The primary antibodies used included anti-CD63 (1:1000, ab68418), anti-CD81 (1:1000, ab109201), anti-CD9 (1:1000, ab223052), anti-CD80 (1:1000, ab134120), anti-CD86 (1:1000, ab239075), anti-CD206 (1:1000, ab64693), anti-CD163 (1:1000, ab182422), anti-p-NF-κB p65 (1:1000, ab267373), anti-NF-κB p65 (1:1000, ab68153), anti-HMGB1 (1:1000, ab179483), and anti-GAPDH (1:1000, ab9485) antibodies. All the antibodies were obtained from Abcam (MA, USA).

2.10. Reverse transcription–polymerase chain reaction (RT–PCR)

TRIzol reagent (Invitrogen, USA) was used to isolate total RNA from macrophages and myocardial tissues. The Superscript First Strand Synthesis System (Invitrogen, USA) was used to reverse transcribe the RNA into cDNA. Real-time quantitative PCR (SYBR Green) and an ABI-7900 sequence detection system (Applied Biosystems, USA) were utilized for real-time PCR. The $2^{-\Delta\Delta CT}$ method was used to calculate the relative profiles of Snhg14 and miR-181a-5p, with β-actin and U6 as internal parameters. The primers used in our study included Snhg14: forward 5′- ACCTGCAAGCTTTTTGACCC-3′, reverse 5′- AGCAGACAAAGAAAAACCCCAAT-3'; miR-181a-5p: forward 5′-ACACTCCAGCTGGGAACATTCAACGCTGTCGG-3′, reverse 5′-TGGTGTCGTGGAGTCG-3'; U6: forward 5′-CTCGCTTCGGCAGCACA-3′, reverse 5′-AACGCTTCACGAATTTGCGT-3'; and β-actin: forward 5′- CCAACCGTGAAAAGATGACC-3′, reverse 5′- CCAGAGGCATACAGGGACAG-3'.

2.11. Construction of the mouse sepsis model

Adult C57/BL/6J mice (8 weeks, 22 ± 2 g in weight), supplied by the Animal Center of Xinjiang Medical University (Urumqi, China), were used in our study. The mice were reared under controlled conditions, with access to food and water. All animal experiments were approved by the Ethics Committee of Shandong University Zibo Central Hospital (approval no: ZBCH-012-2022) and were implemented in line with the Guidelines of the National Institute for Animal Protection and Ethics.

The mice were randomized to the Sham group, the sh-Snhg14 group, the CLP group, or the CLP + sh-Snhg14 group. Ten mice were included in each group. Cecal ligation and puncture (CLP) surgery was conducted to establish a mouse sepsis-induced myocardial damage model [27]. All the mice were fasted for 12 h prior to surgery but were allowed to drink freely. First, the animals were anaesthetized with pentobarbital, and the peritoneum was cut along the midline of the abdomen to expose the cecum under aseptic conditions. A fine thread was used immediately to ligate the middle part of the cecum, and an 18-gauge needle was used to puncture the end of the cecum twice. With a small amount of gastric content squeezed out, the cecum was returned to the abdominal cavity, and the abdomen was sutured. In the Sham group, CLP was spared, but the remaining steps were the same. The lentiviral shRNA targeting Snhg14 was designed and synthesized by GenePharma (Shanghai, China). In the sh-Snhg14 and CLP + sh-Snhg14 groups, the mice received sh-Snhg14 administration via the tail vein injection at a dose of 80 mg/kg for three consecutive days prior to CLP surgery [27, 28]. We calculated the survival rate of the mice in each group. Cardiac functions were evaluated by a Vevo770 small animal echocardiography machine (Visual Sonics Inc.). The parameters included the LV ejection fraction (EF%) and LV fractional shortening (FS %). After the experiment, the animals were euthanized through cervical dislocation after being anaesthetized by inhalation of 40 % CO_2. Heart tissues were harvested for the following experiments.

2.12. Hematoxylin–eosin (HE) staining

Mouse myocardial tissues were fixed with 10 % paraformaldehyde. Later, the tissues were dehydrated with ethanol and xylene, embedded in paraffin, and sliced. Following dewaxing, the sections were flushed with gradient alcohol and distilled water for 5 min, dyed with hematoxylin for 5 min, rinsed in running water for 3 s, washed with 1 % hydrochloric acid ethanol for 3 s, and stained with 5 % eosin for 3 min. After dehydration, the slices were cleaned, and a light microscope was used to observe the histological changes in the myocardial tissues.

2.13. Masson staining

Mouse heart tissues were fixed with 4 % paraformaldehyde, embedded in paraffin, and sliced (4 μm thick). As instructed by the manufacturer, the Masson tricolor staining kit (Cat.No. G1340, Solarbio, Beijing, China) was used for Masson tricolor staining. The sections were treated with hematoxylin and ferric oxide, acid fuchsin, phosphomolybdic acid, and acetic acid, successively. Then, they were sealed with neutral gum. A microscope was used for observation.

2.14. Immunofluorescence and TUNEL staining

Mouse heart tissues were fixed with 4 % paraformaldehyde, embedded in paraffin, and sliced (4 μm thick). The embedded paraffin was immersed in xylene twice. The tissues were flushed with 100 % ethanol twice and dehydrated with gradient ethanol for 3 min. The endogenous catalase and endogenous antigen were blocked with 5 % goat serum. Later, the slices were incubated with the primary antibody anti-Iba1 (Cat.no. 019–19741, Wako Chemicals, Richmond, VA) or Anti-Collagen I (ab270993, Abcam) diluted with 5 % goat serum overnight at 4 °C. The sections were washed with PBS, incubated with goat anti-rabbit IgG H&L (Alexa Fluor® 488) (ab150077) at RT for 120 min, and rinsed with PBS again. The cell nucleus was stained with DAPI. A fluorescence microscope was used to observe the immunohistochemical reactions. A TUNEL Apoptosis Detection Kit (Green Fluorescence, Abbkine, China) was used to measure apoptosis in myocardial cells and tissues. In accordance with the manufacturer's instructions, terminal deoxynucleotidyl transferase (TdT)-labelled reaction buffer was prepared. Next, 50 μl of the reaction mixture was added to each sample for 60 min of culture at 37 °C. The slices were washed with PBS three times, and the nuclei were dyed with 0.05 μg/ml DAPI. The slices were rinsed with PBS three more times. A fluorescence microscope (BX53, Olympus, Japan) was used for observation.
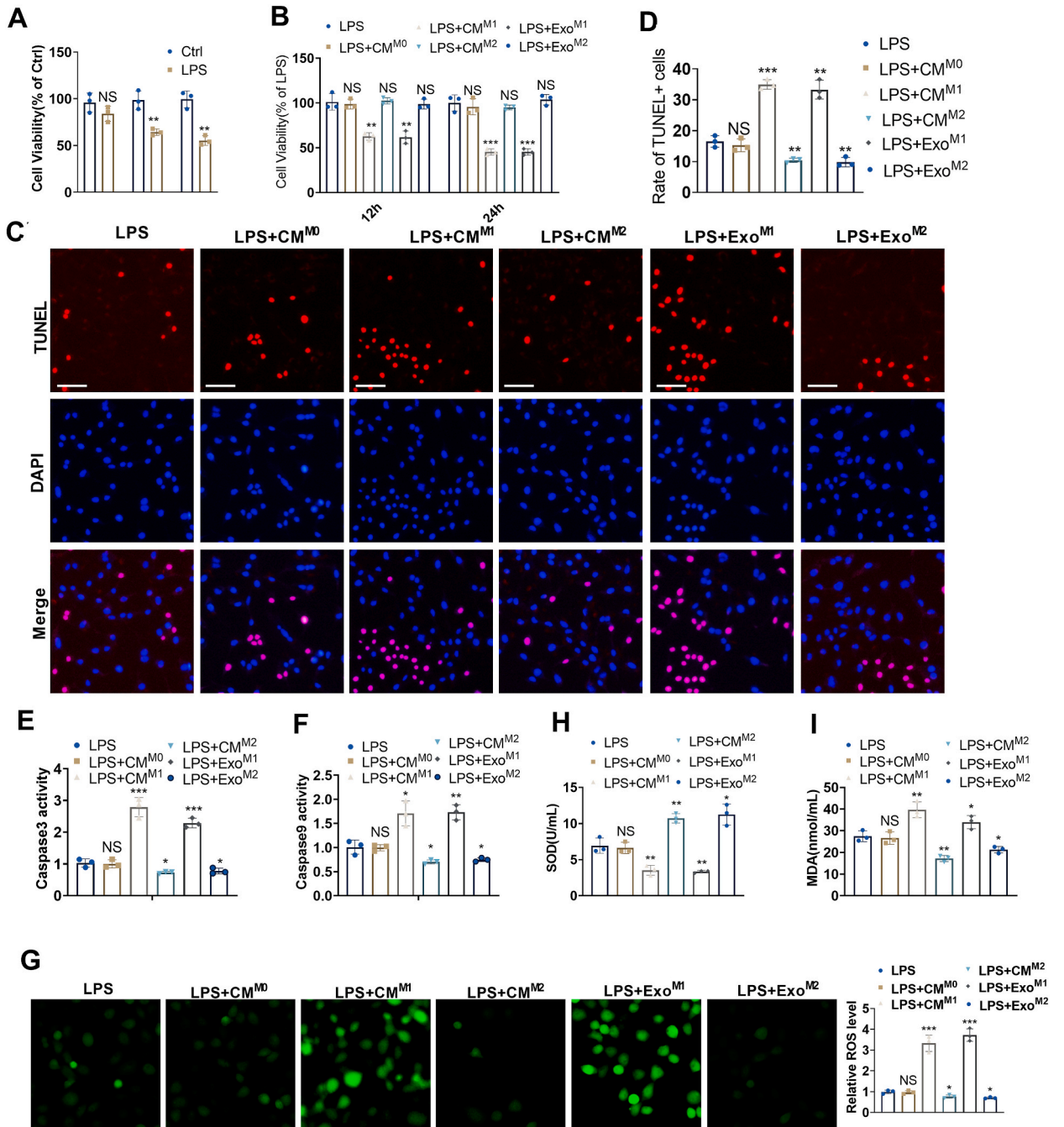
Fig. 1. M1-polarized macrophages bolster LPS-induced myocardial cell damage
A. LPS (5 μg/mL) was used to treat myocardial cells for 24 h and cell viability was determined by CCK8 assay. RAW264.7 cells were differentiated into M0 macrophages, which were then induced to polarize into M1 and M2 macrophages. The conditioned medium or exosomes of the macrophages were used to treat LPS-induced myocardial cells. B. A CCK8 assay was used to examine the viability of myocardial cells. C-D. TUNEL staining was used to evaluate apoptosis in induced myocardial cells. Scale bar = 50 μm. E–F: A Caspase3/9 activity detection kit was used to confirm the activities of Caspase3 and Caspase9 in LPS-induced myocardial cells. G: A DCFDA/H2DCFDA-Cellular ROS assay kit was used to determine the ROS levels in the cells. H–I: Oxidative stress factor detection kits were used to measure SOD and MDA levels in the cells. N = 3. *NS P>0.05, *P<0.05, **P<0.01, ***P<0.001* (vs. the ctrl or LPS group).

2.15. Statistical analysis

GraphPad Prism 8.0 software was used for statistical analysis. All the data are presented as the means ± standard deviations. Independent Student's *t*-test was used to compare two groups, whereas one-way ANOVA was adopted for comparisons among multiple groups. The Kaplan–Meier method was utilized to evaluate the survival of the mice. *P < 0.05* was regarded as statistically significant.

3. Results

3.1. "M1" polarized macrophages increased LPS-induced myocardial cell damage

PMA was administered to differentiate RAW264.7 cells into M0 macrophages. M0 macrophages were then incubated with 20 ng/mL IFN-γ+10 pg/mL LPS for 48 h to produce M1 macrophages. Moreover, M0 macrophages were incubated with 20 ng/mL IL-4+20 ng/mL IL-13 for 48 h to produce M2 macrophages. ELISA confirmed the profiles of proinflammatory and anti-inflammatory cytokines
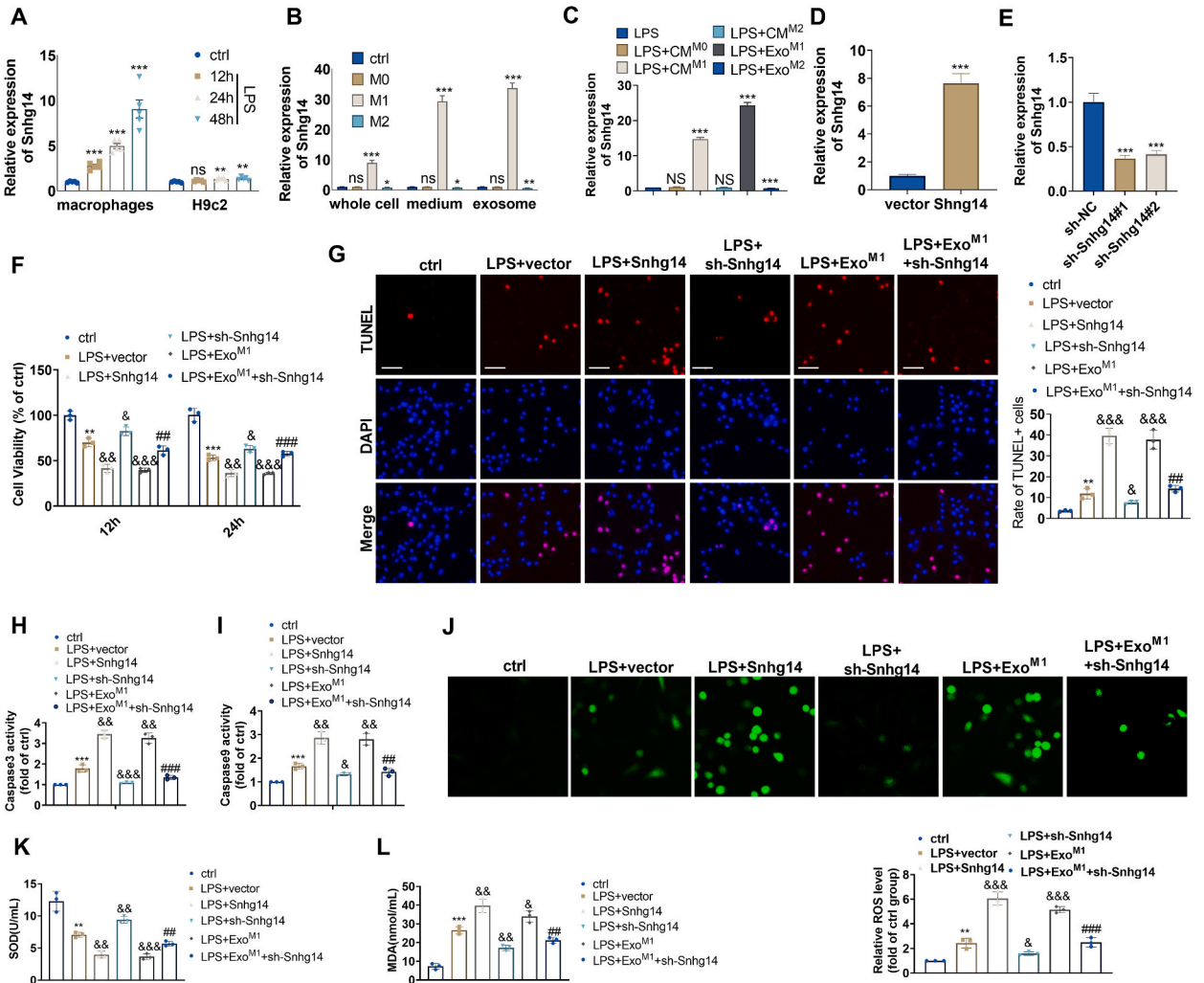

Fig. 2. The role of Snhg14 in LPS-elicited myocardial cell damage
A. RAW264.7 cells or H9c2 cells were treated with LPS (5 μg/mL) for different durations. The level of Snhg14 in the two cells was tested by RT–PCR. B. RAW264.7 cells were polarized into different phenotypes (M1 and M2). The level of Snhg14 in the cells, medium and exosomes was tested by RT–PCR. N = 3. *ns P>0.05, *P<0.05, **P<0.01, ***P<0.001* (vs. the ctrl group). C. H9c2 cells were treated with CM or exosomes from M1/M2 macrophages then the Snhg14 level was tested by RT-PCR. D-E. H9c2 cells were transfected with Snhg14 overexpression plasmids or sh-Snhg14. F. A CCK-8 assay was used to examine the viability of LPS-induced myocardial cells. G: TUNEL staining was used to evaluate apoptosis in induced myocardial cells. Scale bar = 50 μm. H–I: A Caspase3/9 activity detection kit was used to confirm the activities of Caspase3 and Caspase9 in LPS-induced myocardial cells. J A DCFDA/H2DCFDA-Cellular ROS assay kit was used to determine the ROS levels in the cells. K–L: Oxidative stress factor detection kits were used to measure SOD and MDA levels in the cells. N = 3. **P<0.01, ***P<0.001* (vs. ctrl group). *&P<0.05, &&<0.01, &&&P<0.001* (vs. LPS + vector group). *##<0.01, ###P<0.001* (vs. LPS + Exo^M1 group).
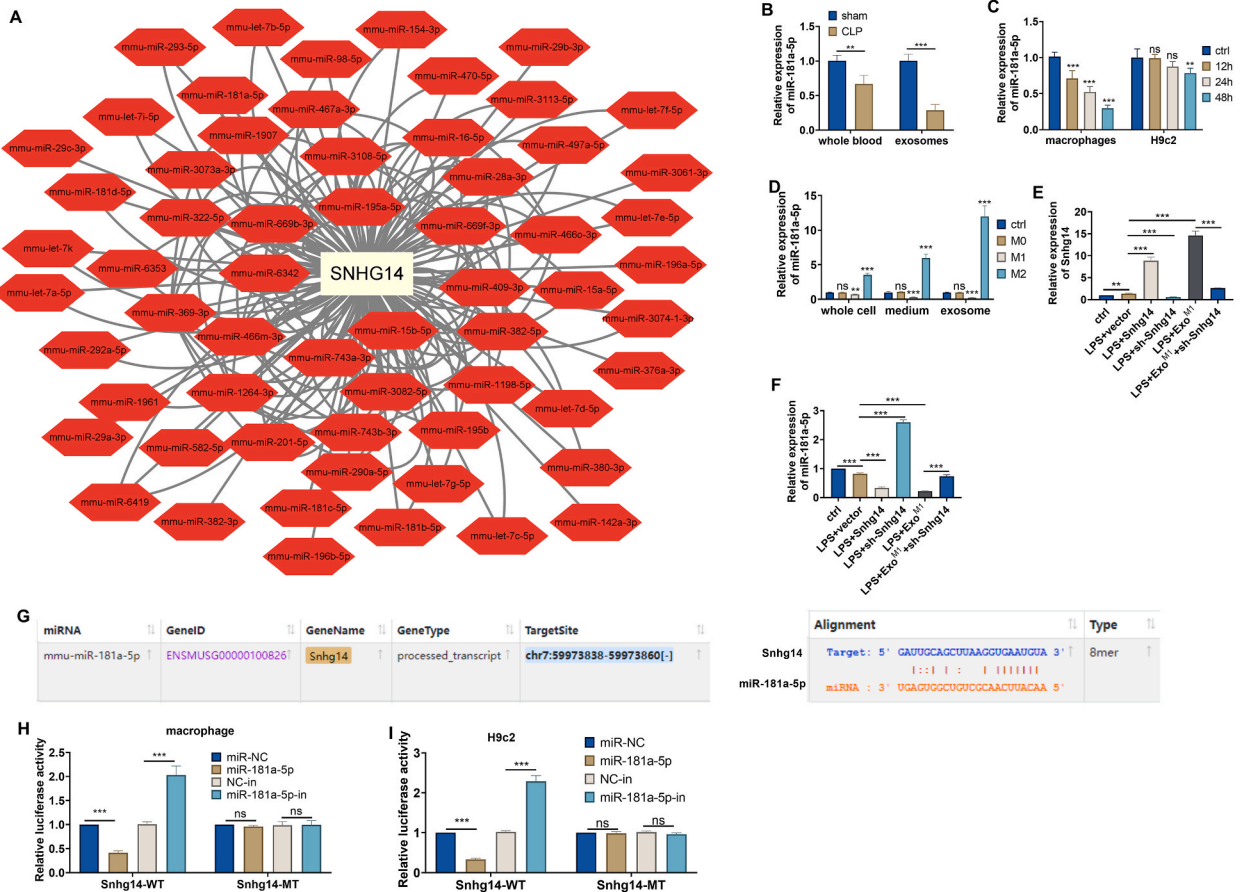
Fig. 3. Snhg14 targeted and negatively regulated miR-181a-5p
A. The miRNA targets of Snhg14 via ENCORI (https://rnasysu.com/encori/). The Snhg14-miRNA network is shown. B. The levels of miR-181a-5p in the whole blood and blood-derived exosomes of CLP mice were tested via RT–PCR. C. RAW264.7 cells or H9c2 cells were treated with LPS (5 μg/mL) for different durations. The level of miR-181a-5p in the cells was tested via RT–PCR. D. RAW264.7 cells were polarized into different phenotypes (M0, M1, and M2). H9c2 cells were transfected with Snhg14 overexpression plasmids or sh-Snhg14. E–F. The levels of Snhg14 (E) and miR-181a-5p (F) in the cells were tested by RT–PCR. Next, the level of miR-181a-5p in the blood and cells was tested. G. The base-binding relationship between Snhg14 and miR-181a-5p is shown. H-I. A dual-luciferase reporter gene assay was conducted to confirm the targeting relationship between Snhg14 and miR-181a-5p. N = 3. NS P > 0.05, **P < 0.01, ***P < 0.001.

in the macrophages (Sup Figure A). We used LPS (5 μg/mL) to induce damage to myocardial cells. The results of the CCK-8 assay revealed that, in contrast with that of the Ctrl group, the viability of the LPS-induced myocardial cells was significantly decreased (Fig. 1A). CM or exosomes from M1/M2 macrophages were collected and used to treat myocardial cells. Compared with that in the LPS group, cell viability in the LPS + CM^{M1} group and the LPS + Exo^{M1} group was significantly lower than that in the LPS group but not in the LPS + CM^{M2} group or the LPS + Exo^{M2} group (Fig. 1B). TUNEL staining suggested that CM^{M1} and Exo^{M1} administration aggravated myocardial cell apoptosis. By contrast, the treatment of CM^{M2} and Exo^{M2} markedly attenuated the TUNEL-positive cell rate (vs. the LPS group, Fig. 1C–D). The activities of Caspase3 and Caspase9 were increased in the LPS + CM^{M1} group and the LPS + Exo^{M1} group, and attenuated in the LPS + CM^{M2} and LPS + Exo^{M2} group (vs. the LPS group, Fig. 1E–F). In contrast to those in the LPS group, the levels of both ROS and MDA were elevated, whereas the SOD level was reduced in the LPS + CM^{M1} group and the LPS + Exo^{M1} group (vs. the LPS group, Fig. 1G–I). On the contrary, CM^{M2} and Exo^{M2} treatment significantly reduced ROS and MDA levels and enhanced SOD level (vs. the LPS group, Fig. 1G–I). These findings confirmed that "M1" polarized macrophages bolster LPS-elicited myocardial cell damage.

3.2. Snhg14 knockdown reversed M1-MΦ-exo-induced myocardial cell damage

Following LPS treatment, Snhg14 levels in RAW264.7 cells and H9c2 cells were assessed by RT-PCR. The data showed that Snhg14 level was increased in the two cells, especially in RAW264.7 cells (Fig. 2A). The Snhg14 level in the CM and exosomes of RAW264.7 cells was prominently increased (vs. the ctrl group, Fig. 2B). In addition, the Snhg14 level had a significant augment in H9c2 cells treated with CM^{M1} or Exo^{M1} (vs. the LPS group, Fig. 2C). To investigate the role of Snhg14 in myocardial cell damage, its overexpression and knockdown models were constructed in H9c2 cells (Fig. 2D–E). Exosomes in the condition medium of MΦs were

isolated and identified by Western blot (Sup Fig. 2A). The size distribution plot showed that about 84.32 % of vesicles have a size between 40 and 100 nm, suggesting that most of the isolated vesicles are exosomes (Sup Fig. 2B–C). H9c2 cells were then treated with Exo^{M1}. Compared with that in the LPS + vector group, cell viability in the LPS + Snhg14 group and the LPS + Exo^{M1} group was lower, and the viability of the LPS + sh-Snhg14 group was greater. Compared with the LPS + Exo^{M1} group, the LPS + Exo^{M1}+sh-Snhg14 group presented increased cell viability (Fig. 2F). The level of H9c2 cell apoptosis was tested. The results revealed that the percentage of TUNEL-positive cells and the activities of Caspase3 and Caspase9 were elevated after Snhg14 overexpression or Exo^{M1} treatment. In contrast, sh-Snhg14 transfection reduced the number of apoptotic cells compared with that in the LPS + vector group or the LPS + Exo^{M1} group (Fig. 2G–I). The oxidative stress levels of H9c2 cells were tested, and the results revealed that Snhg14 overexpression or Exo^{M1} treatment increased the ROS and MDA levels, whereas the SOD level decreased. In contrast, the ROS and MDA levels were reduced following Snhg14 downregulation (compared with those in the LPS + vector group or the LPS + Exo^{M1} group, Fig. 2J–L). These findings demonstrated that "M1"-polarized macrophage-derived exosomes promoted myocardial cell damage induced by LPS.

3.3. Snhg14 targeted and negatively regulated miR-181a-5p

To further investigate the mechanism by which Snhg14 mediates macrophage polarization and myocardial cell damage, we searched for the miRNA targets of Snhg14 via ENCORI (https://rnasysu.com/encori/). The Snhg14-miRNA network is shown in Fig. 3A. Next, the level of miR-181a-5p in the blood and cells was tested. The results revealed that miR-181a-5p was downregulated in whole blood and blood exosomes (Fig. 3B). LPS treatment led to reduced expression of miR-181a-5p in macrophages and H9c2 cells (Fig. 3C). In addition, the miR-181a-5p level was reduced in the culture medium and exosomes of M1-polarized macrophages (Fig. 3D). In H9c2 cells, Snhg14 was promoted after Snhg14 overexpression and M1-Exo treatment (Fig. 3E). The opposite trend was observed for the miR-181a-5p level, and Snhg14 knockdown increased miR-181a-5p expression (Fig. 3F). The base-binding relationship between Snhg14 and miR-181a-5p is shown in Fig. 3G. A dual-luciferase reporter gene assay suggested that miR-181a-5p mimics attenuated the luciferase activity of cells transfected with the Snhg14 wild-type (WT) 3′-UTR and that miR-181a-5p inhibitors enhanced the luciferase activity of cells transfected with Snhg14-WT. However, miR-181a-5p mimics and miR-181a-5p inhibitors had no significant effects on the luciferase activity of cells transfected with the Snhg14-mutant type (Snhg14-MT) (Fig. 3H–I). Thus, miR-181a-5p is a target of Snhg14.

3.4. The impact of the Snhg14/miR-181a-5p axis on macrophage polarization

To explore the influence of the Snhg14/miR-181a-5p axis on macrophage polarization, Snhg14 overexpression plasmids, sh-Snhg14, miR-181a-5p mimics, and miR-181a-5p inhibitors were used to transfect macrophages. RT–PCR revealed that Snhg14 overexpression attenuated miR-181a-5p levels and that sh-Snhg14 promoted miR-181a-5p levels. However, miR-181a-5p had a weaker effect on Snhg14 expression (P > 0.05, Fig. 4A–D). As indicated by ELISA, Snhg14 overexpression and miR-181a-5p inhibition enhanced the profiles of TNF-α, IL-1β, IL-6, and IL-10 in macrophages, whereas Snhg14 knockdown and miR-181a-5p overexpression decreased the profiles of TNF-α, IL-1β, and IL-6 and increased IL-10 expression. Compared with the Snhg14 group, the Snhg14+miR-181a-5p group presented a reduction in the profile of proinflammatory cytokines and an increase in the profile of anti-inflammatory cytokines in macrophages. In contrast with those in the sh-Snhg14 group, the levels of TNF-α, IL-1β, IL-6, and IL-10 in the sh-Snhg14 + miR-181a-5p-in group increased (Fig. 4E and G). Compared with the corresponding control groups, Snhg14 overexpression, and miR-181a-5p inhibition augmented CD80 and CD86 expression and attenuated CD206 and CD163 expression in macrophages, whereas Snhg14 knockdown and miR-181a-5p overexpression reversed these effects. In contrast to the Snhg14 group, the Snhg14+miR-181a-5p group presented decreases in CD80 and CD86 expression and increases in CD206 and CD163 expression in macrophages. In contrast with those in the sh-Snhg14 group, CD80 and CD86 expression was upregulated, whereas CD206 and CD163 expression was downregulated in the sh-Snhg14 + miR-181a-5p-in group (Fig. 4G and H). These findings confirmed that Snhg14 overexpression bolstered the M1 polarization of macrophages, whereas miR-181a-5p overexpression suppressed this polarization.

3.5. miR-181a-5p overexpression reversed the effects of M1 macrophages on LPS-induced myocardial cell damage

To understand the function of miR-181a-5p in myocardial cell damage mediated by Snhg14 or M1-MΦ-exo, we transfected miR-181a-5p mimics into H9c2 cells with Snhg14 overexpression or M1-MΦ-exo treatment (Fig. 5A). The CCK8 assay revealed that, in contrast with the LPS + Snhg14 group or the LPS + Exo^{M1} group, cell viability was dramatically increased (Fig. 5B). TUNEL staining revealed that miR-181a-5p overexpression reduced the percentage of TUNEL-positive myocardial cells (Fig. 5C). Similar results were found after detecting Caspase3 and Caspase9 levels (Fig. 5D–E). Cell immunofluorescence and oxidative stress factor detection kits revealed that, in contrast with those in the control groups, the ROS and MDA levels and SOD levels were lower in the LPS-induced myocardial cells than in the control groups (Fig. 5F–H). After miR-181a-5p mimic transfection, both ROS and MDA levels were reduced, and SOD levels were increased (Fig. 6F–H). These findings demonstrated that miR-181a-5p weakened the ability of M1 macrophages to promote LPS-induced myocardial cell damage.

3.6. Downregulating Snhg14 increased the survival rate of septic mice

To better understand the function of Snhg14 in sepsis-induced myocardial injury, we carried out CLP to construct a mouse sepsis model via transfection with sh-Snhg14. Compared with that of the sham group, the survival rate of the CLP group was distinctly lower,
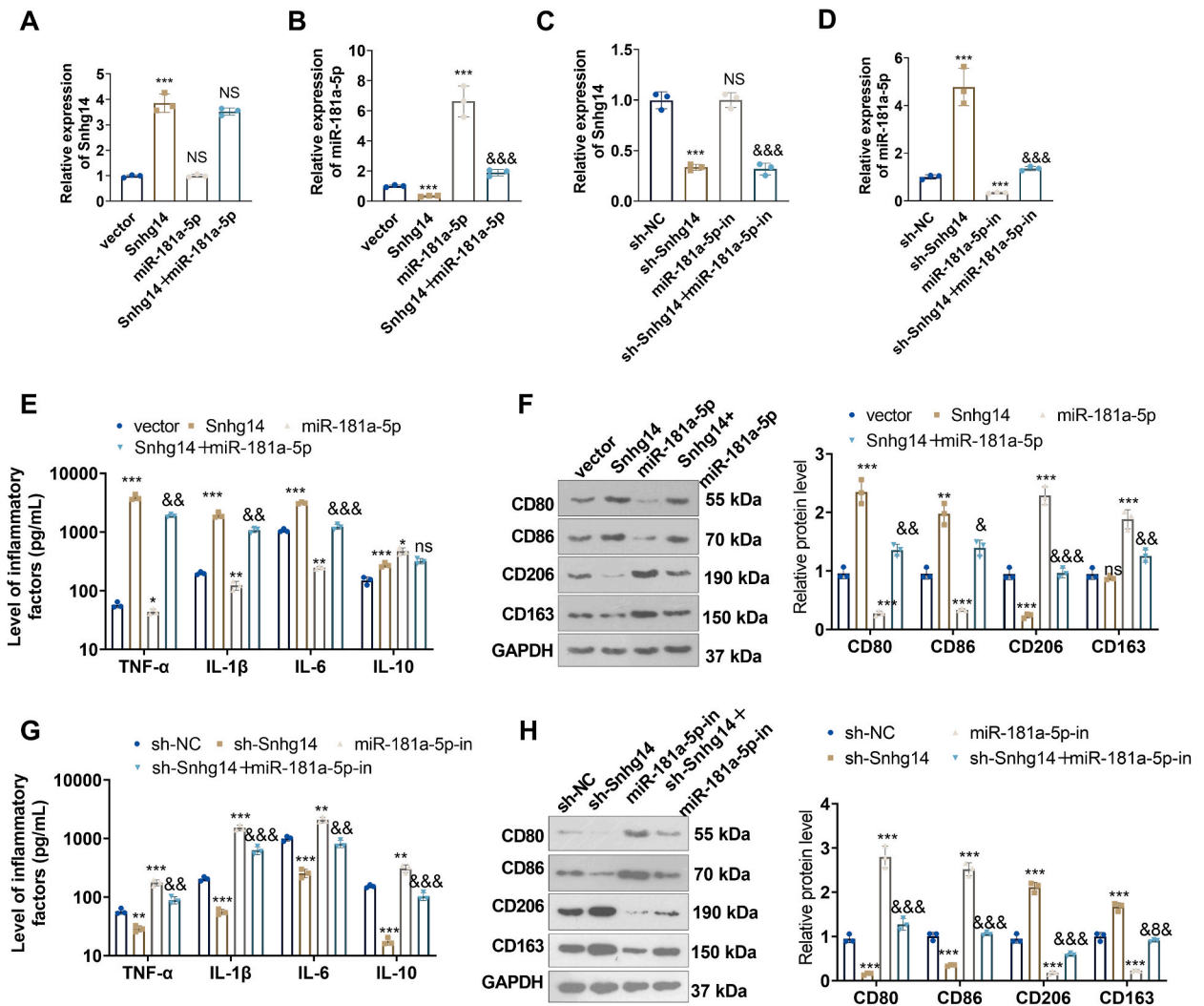
Fig. 4. The impact of the Snhg14/miR-181a-5p axis on macrophage polarization.
Snhg14 overexpression plasmids, sh-Snhg14, miR-181a-5p mimics, and miR-181a-5p inhibitors were used to transfect macrophages. A–D. RT–PCR was used to test Snhg14 and miR-181a-5p levels. E. ELISA was used to test the profiles of TNF-α, IL-1β, IL-6, and IL-10 in macrophages. F. Western blotting was conducted to test CD80, CD86, CD206 and CD163 expression in macrophages. G. ELISA was used to test the profiles of TNF-α, IL-1β, IL-6, and IL-10 in macrophages. H. Western blotting was conducted to test CD80, CD86, CD206 and CD163 expression in macrophages. N = 3. *ns P > 0.05, *P < 0.05, **P < 0.01, ***P < 0.001* (vs. vector or group). *ns P > 0.05, &P < 0.05, && < 0.01, &&&P < 0.001* (vs. ctrl group)

and sh-Snhg14 markedly elevated the survival rate of the CLP group (Fig. 6A). The echocardiogram revealed that EF (%) and FS (%) were not significantly altered in the sh-Snhg14 group, whereas the CLP group presented significant decreases in EF (%) and FS (%). Notably, the echocardiogram examination showed that compared with the CLP group, the CLP mice with Snhg14 knockdown led to an increment in EF (%) and FS (%) (Fig. 6B–D). HE staining, Masson's trichrome staining and immunofluorescence revealed that, in contrast with that in the CLP group, pathological injury to the myocardial tissues of the CLP + sh-Snhg14 group was dramatically mitigated, coupled with lower levels of collagen deposition (Fig. 6E and 7A–B). Furthermore, the TUNEL staining revealed that, in contrast with the sham group, the CLP group presented a substantial increase in TUNEL-positive cell rate. sh-Snhg14 treatment reduced the TUNEL-positive cell rate in comparison to that of the CLP group (p < 0.05), indicating that sh-Snhg14 treatment represses apoptosis (Fig. 7C). These findings confirmed that M1 macrophage exosomes transfected with sh-Snhg14 increased the survival rate of septic mice and inhibited apoptosis.

3.7. Knocking down Snhg14 repressed macrophage activation, inflammation and oxidative stress in the myocardial tissues of septic mice

Immunofluorescence was conducted to detect Iba1-labelled macrophages in the heart tissues. Compared with the sham group, the number of macrophages labelled with Iba1 was greater in the myocardial tissues of CLP mice, whereas sh-Snhg14 treatment mitigated
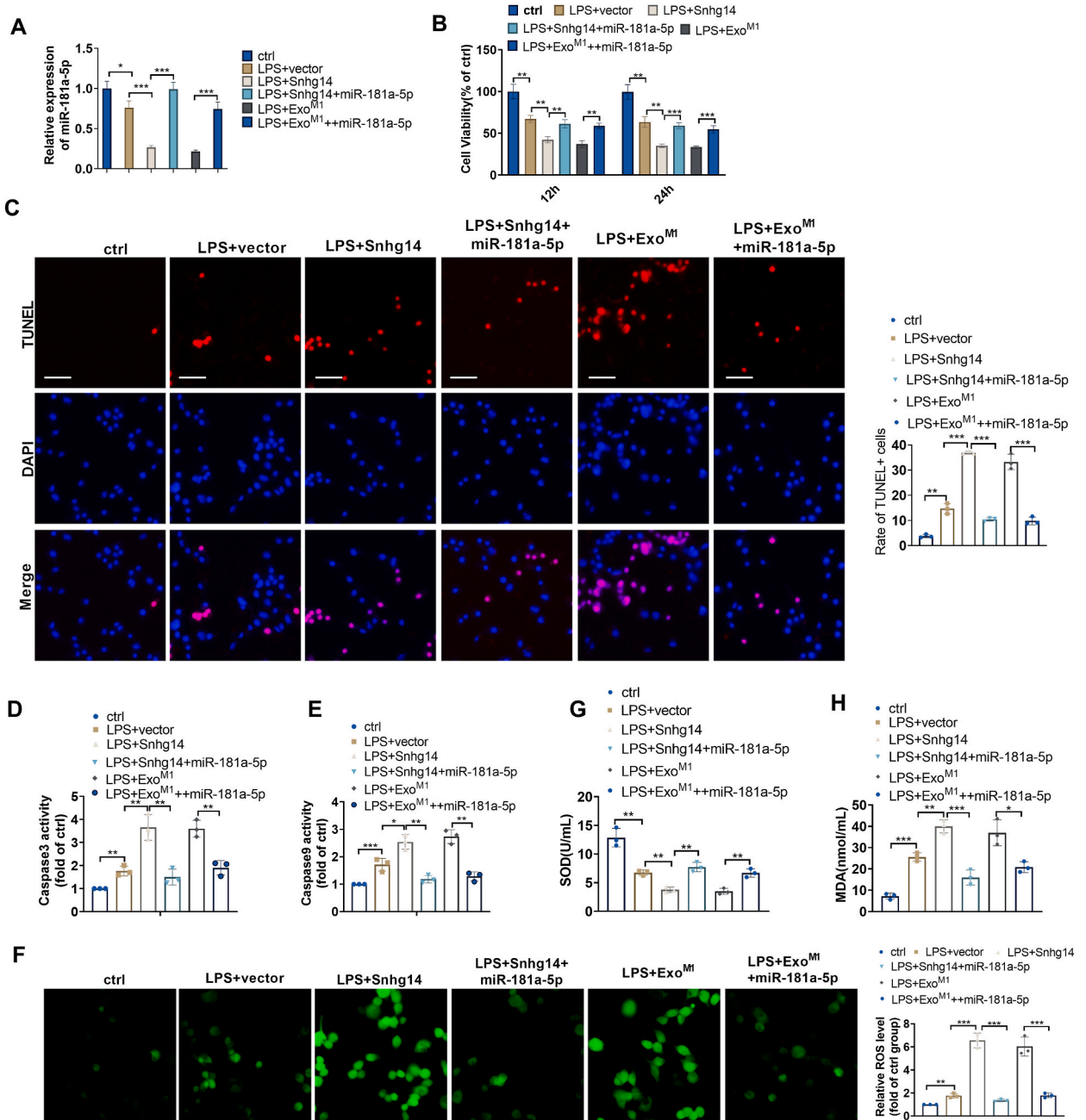
Fig. 5. miR-181a-5p overexpression reversed M1-polarized macrophage-elicited myocardial cell damage
M1 macrophage-derived exosomes were used to treat LPS-induced myocardial cells transfected with miR-181a-5p mimics. A. RT−PCR was used to test the miR-181a-5p levels. B: A CCK8 assay was used to examine the viability of LPS-induced myocardial cells. C: TUNEL staining was used to measure apoptosis in the cells. D−E: A Caspase3/9 activity detection kit was used to confirm the activities of Caspase3 and Caspase9 in LPS-induced myocardial cells. F: A DCFDA/H2DCFDA-Cellular ROS assay kit was used to determine the ROS levels in the cells. G-H: Oxidative stress factor detection kits were used to measure SOD and MDA levels in the cells. N = 3. *P < 0.05, **P < 0.01, ***P < 0.001.

the infiltration of Iba1-labelled macrophages in the tissues compared with the CLP group (p < 0.01, Fig. 8A). ELISA and oxidative stress factor detection kits were used to verify the alterations of inflammatory and oxidative stress factors in the myocardial tissues. Compared with those in the CLP group, the levels of TNF-α, IL-1β, IL-6, and MDA were greatly reduced, whereas the level of SOD was decreased in the myocardial tissues of mice in the CLP + sh-Snhg14 group (Fig. 8B–F). RT−PCR and western blotting revealed that, in contrast with the sham group, the CLP group presented increased Snhg14 expression and decreased miR-181a-5p expression. In contrast to the CLP group, sh-Snhg14 treatment inhibited Snhg14 level, increased miR-181a-5p expression, and impeded the
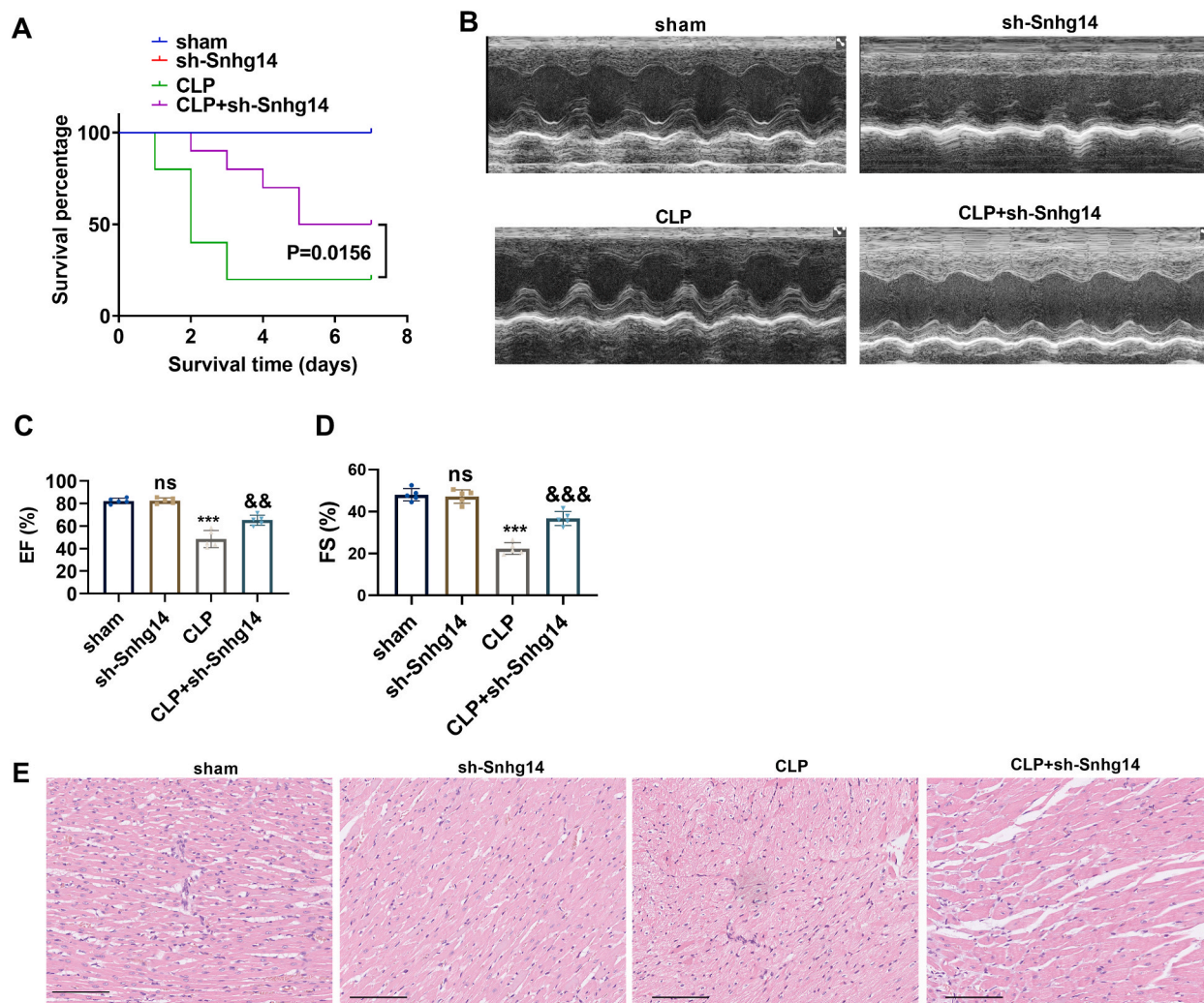
Fig. 6. sh-Snhg14 increased the survival rate of septic mice

A mouse sepsis model was constructed, and sh-Snhg14 was used to downregulate Snhg14. A: The survival rates of the mice in each group were compared. B. Cardiac functions were evaluated via a Vevo770 small animal echocardiography machine. C-D. The parameters included the LV ejection fraction (EF%) and LV fractional shortening (FS%). E: HE staining was used to measure pathological alterations in mouse myocardial tissues. N = 5. *ns P>0.05, ***P<0.001* (vs. Sham); *&&P<0.01, &&&P<0.001* (vs. CLP).

expression of HMGB1 and the p-NF-κB pathway in myocardial tissues of CLP mice (Fig. 8G–I, Supplementary Fig. 3). These results demonstrated that downregulating sh-Snhg14 dampened HMGB1/NF-κB expression and enhanced miR-181a-5p in the myocardial tissues of mice with sepsis.

4. Discussion

The incidence and mortality rates of sepsis are high. The heart is one of the most vulnerable organs. Sepsis combined with myocardial damage may exacerbate the disease and increase the likelihood of multiple organ failure and death [29,30]. Our study investigated the role of M1 macrophages in increasing sepsis-induced myocardial damage via the Snhg14/miR-181a-5p axis. We discovered that exosomes derived from M1 macrophages express miR-181a-5p via the lncRNA Snhg14, exacerbating LPS-induced myocardial cell damage.

Macrophages are significant components of innate and adaptive immunity. In the context of sepsis, inflammatory responses are dysregulated, and macrophages are recruited to the heart, where they polarize into M1 and M2 macrophages in different microenvironments and under different stimulating factors [31,32]. Under LPS stimulation, bone marrow-derived macrophages release proinflammatory cytokines and cause myocardial impairment [33]. Recently, exosomes derived from polarized macrophages have been shown to play a significant role in the pathophysiological process of sepsis-induced myocardial injury. For example, the M2 macrophage exosome microRNA-24-3p downregulates tumor necrosis factor superfamily member 10 (Tnfsf10) expression to alleviate
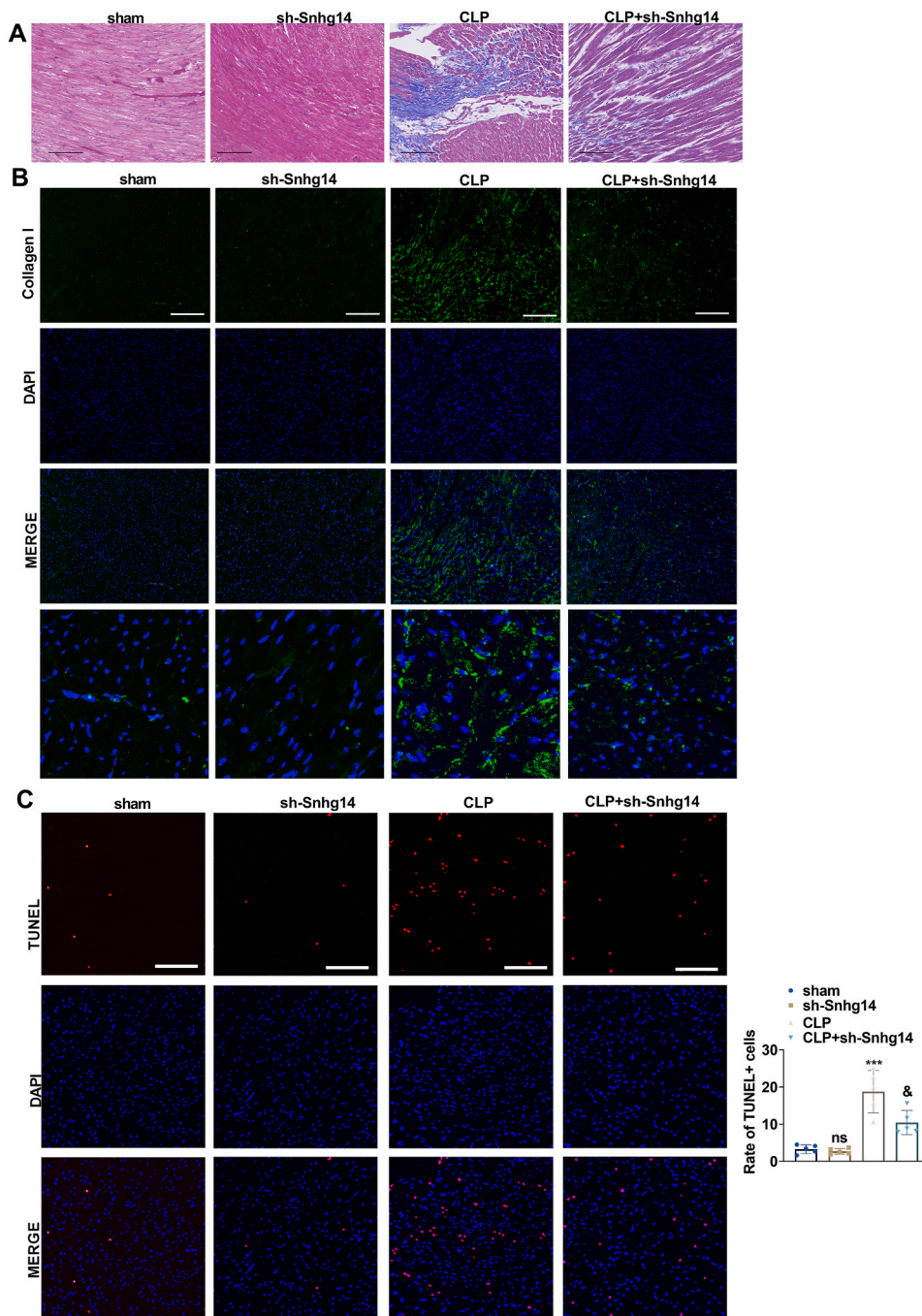
Fig. 7. sh-Snhg14 inhibited the in mouse myocardial tissues

A.Masson's trichrome staining were used to measure pathological alterations in mouse myocardial tissues. B. Collagen I expression was tested by immunofluorescence. C: TUNEL staining was used to evaluate apoptosis in mouse myocardial tissues and cells. N = 5. *ns P>0.05, ***P<0.001* (vs. Sham); *&P<0.05* (vs. CLP).

myocardial damage in LPS-induced septic mice [34]. Interleukin-12a (IL12a) and interleukin-5 (IL-5) gene knockout can elicit the M1 polarization of macrophages to exacerbate myocardial damage in LPS-induced septic mice [35,36]. Here, we established an *in vitro* sepsis-induced myocardial injury model. We discovered that, in contrast with the corresponding control groups, M1 macrophages and their exosomes considerably increased apoptosis, oxidative stress, and inflammatory responses in LPS-induced myocardial tissues. These findings suggest that M1 macrophages aggravate sepsis-induced myocardial injury.
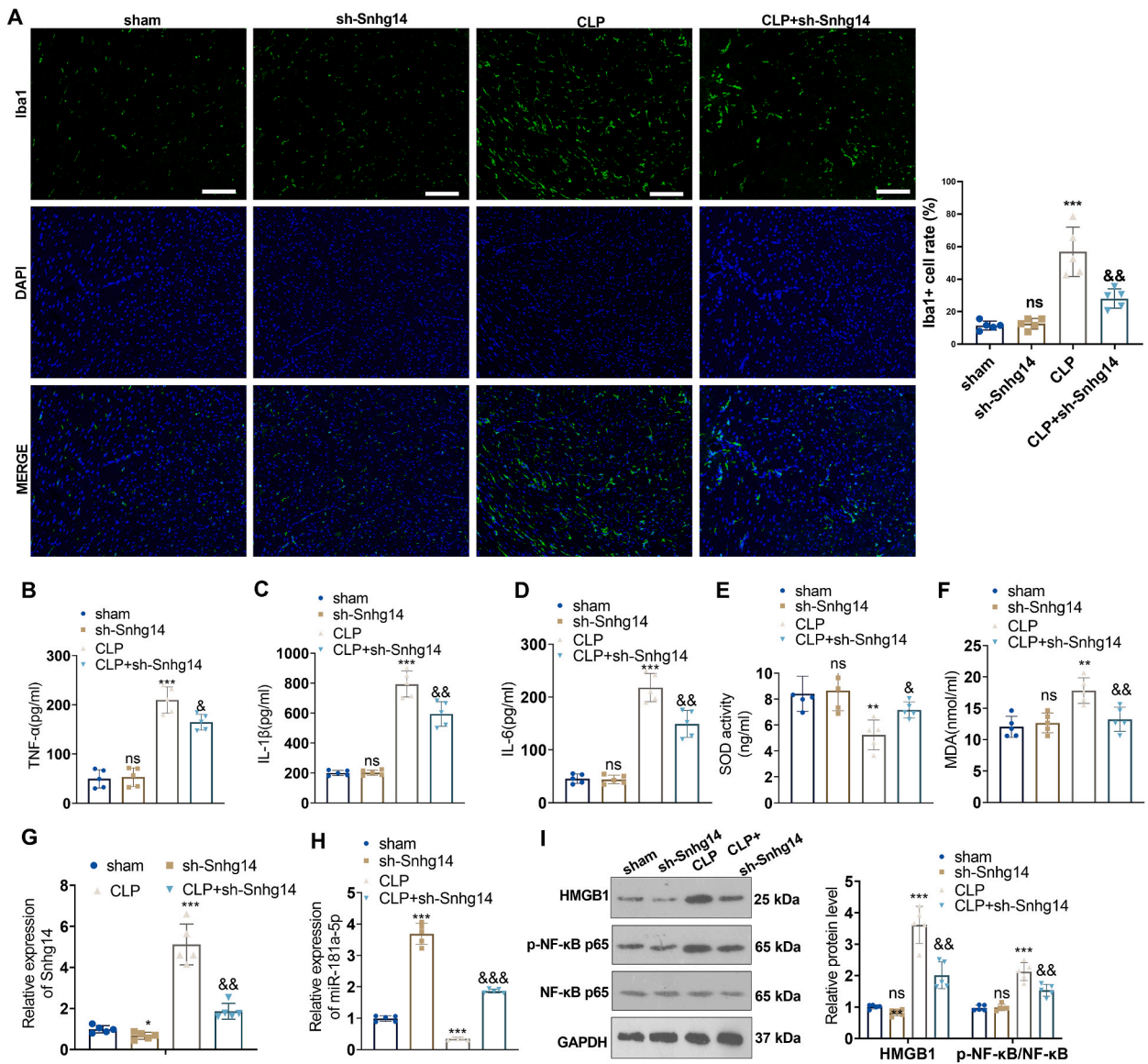
Fig. 8. sh-Snhg14 dampened macrophage activation, inflammation and oxidative stress in the myocardial tissues of septic mice
A. The activation of macrophages (labelled with Iba1) was tested by immunofluorescence. B–D: ELISA confirmed the profiles of TNF-α, IL-1β, and IL-6 in the myocardial tissues of the mice. E–F: Oxidative stress factor detection kits were used to verify the SOD and MDA levels in the tissues. G–H: RT–PCR was used to determine the profiles of Snhg14 and miR-181a-5p. I. Western blot analysis of the HMGB1/NF-κB pathway in cardiac tissues. N = 3. *P < 0.05, **P < 0.01, ***P < 0.001 (vs. Sham); &P < 0.05, &&P < 0.01, &&&P < 0.001 (vs. CLP).

LncRNAs have been shown to participate in the pathogenesis of sepsis [37]. For example, lncRNA-Cox2 knockdown hampers the CREB-C/EBPβ signalling pathway to attenuate macrophage M1 polarization and inflammation, hence relieving sepsis in mice [38]. LncRNA PVT1 knockdown upregulated microRNA-29a and restrained HMGB1 expression to weaken the M1 polarization of macrophages, thereby mitigating myocardial damage in LPS-induced septic mice [39]. Several members of the SNHG family, such as SNHG1 [40] and SNHG5 [41], have been found to perform pivotal functions in the progression of sepsis. SNHG14 has elevated expression in the plasma of sepsis patients, and it aggravates the cellular damage to and inflammation of kidney cells under LPS stimulation [42]. Moreover, SNHG14 can also be shuttled by exosomes from breast cancer cells, and exosomal SNHG14 promotes the transformation of activated normal fibroblasts to cancer-associated fibroblasts, thus aggravating breast cancer progression [43]. In this study, we found that macrophages had significantly elevated Snhg14 expression after LPS stimulation. Though Snhg14 was only slightly upregulated in H9c2 cells, functional assays confirmed that Snhg14 overexpression aggravated LPS-mediated H9c2 cell damage and Snhg14 down-regulation relieved LPS-mediated H9c2 cell damage. Those data supported that Snhg14 is involved in myocardial cell damage in sepsis. Further experimental data showed that H9c2 cells gained a much higher Snhg14 level when treated with the condition medium or exosomes from "M1" macrophages. Since macrophages had much higher Snhg14 level, we guessed that in the sepsis model, myocardial

cells gained exogenous Snhg14 from macrophages. Higher Snhg14 level in myocardial cells can aggravate LPS-mediated cell damage. In macrophages, LPS stimulation can not only enhance Snhg14 expression but also promote proinflammatory cytokines (eg. IL-1β , IL-6, TNF-α), and the later can meanwhile induce myocardial cell injury. Knocking down Snhg14 mitigated M1 macrophage polarization and ameliorated apoptosis, inflammation, and oxidative stress in myocardial cells. Cardioprotective effects were also observed in septic mice after Snhg14 downregulation. Therefore, these data revealed that Snhg14 is a potential therapeutic target in sepsis-induced heart damage.

Through bioinformatic analysis, we found that miR-181a-5p is a downstream target of Snhg14. Similarly, long noncoding RNA small nucleolar RNA host gene 1 (SNHG1) restrains miR-181a-5p expression and upregulates X-linked inhibitor of apoptosis protein (XIAP) to defend myocardial cells from LPS-induced sepsis-induced myocardial injury [44]. lncRNA CRNDE knockdown upregulated miR-181a-5p and repressed NF-κB activation and the generation of inflammatory factors (TNF-α, IL-1β, and IL-6) in LPS-induced THP-1 cells, hence ameliorating the inflammatory response to sepsis [45]. Current evidence indicates that HMGB1, which is a nuclear protein found in most cells, has crucial roles in various human pathological and pathophysiological processes, such as the inflammatory response, immune reactions, cell migration, aging, and cell death. Suppression of HMGB1 might lead to improved patient outcomes by reducing inflammation [46]. HMGB1 is capable of activating TLR4 through MyD88-or non-MyD88-dependent signalling, thereby initiating downstream signals. Furthermore, it can induce the secretion of inflammatory cytokines via the NF-κB, MAPK, or PI3K pathway [47–49]. Here, we discovered that miR-181a-5p overexpression suppressed macrophage M1 polarization and weakened the toxic impact of M1 macrophage-derived exosomes on LPS-induced myocardial cells. Following Snhg14 downregulation, miR-181a-5p levels are elevated, and the HMGB1/NF-κB pathway is repressed. These findings demonstrated that M1 macrophages increase myocardial damage induced by sepsis by modulating the Snhg14/miR-181a-5p axis.

Several limitations remain in the current work. First, the upstream mechanism of Sngh14 expression in macrophage is unidentified, and the downstream of miR-181a-5p in mediating the HMGB1/NF-κB pathway needs further investigation. Second, the CLP mice received prophylactic treatment of sh-Snhg14 and it is necessary to confirm the therapeutic effects of sh-Snhg14 administration after the CLP procedure. the patterns of macrophages producing exosomes and cardiomyocytes uptaking those exosomes in sepsis require experimental verification. Clinically, the SNHG14/miR-181a-5p/HMGB1/NF-κB axis and exosomal SNHG14 in the serum are potential biomarkers and targets for diagnosing, prognosis, and treating sepsis-associated myocardial damage. However, the mechanisms of septic complications are complex. More clinical samples are needed to further confirm the impacts of those molecules on the clinical practice of sepsis.

5. Conclusions

Overall, our research revealed that the M1 macrophage-derived exosomal Snhg14 restrains miR-181a-5p expression and then initiates the HMGB1/NF-κB pathway, hence increasing the degree of myocardial damage induced by sepsis. For the first time, we demonstrated that the Snhg14/miR-181a-5p axis plays a significant role in sepsis-induced myocardial injury mediated by M1 macrophages. Our findings may provide new approaches and novel targets for diagnosing and treating sepsis-induced myocardial injury.

Funding

Ethics statement

This study was approved by the Ethics Review Board of Shandong University Zibo Central Hospital (Approval No. ZH-EC-2022-122).

Data availability statement

The datasets used and analysed during the current study are available from the corresponding author upon reasonable request.

CRediT authorship contribution statement

Chenglong Bi: Methodology, Investigation. **Dejin Wang:** Software, Data curation. **Bin Hao:** Writing – original draft, Visualization, Resources. **Tianxiao Yang:** Writing – review & editing, Writing – original draft, Supervision.

Declaration of competing interest

The authors declare that they have no known competing financial interests or personal relationships that could have appeared to influence the work reported in this paper.

Acknowledgements

Appendix A. Supplementary data

Supplementary data to this article can be found online at https://doi.org/10.1016/j.heliyon.2024.e37104.

References

[1] A. Sharma, K. Kontodimas, M. Bosmann, The MAVS immune recognition pathway in viral infection and sepsis, Antioxid Redox Signal 35 (16) (2021 Dec) 1376–1392.
[2] S.M. Hollenberg, M. Singer, Pathophysiology of sepsis-induced cardiomyopathy, Nat. Rev. Cardiol. 18 (6) (2021 Jun) 424–434.
[3] Y. Kakihana, T. Ito, M. Nakahara, K. Yamaguchi, T. Yasuda, Sepsis-induced myocardial dysfunction: pathophysiology and management, J Intensive Care 4 (2016 Mar 23) 22.
[4] X. Chen, Y. Liu, Y. Gao, S. Shou, Y. Chai, The roles of macrophage polarization in the host immune response to sepsis, Int. Immunopharm. 96 (2021 Jul) 107791.
[5] J. Chen, J. Lai, L. Yang, G. Ruan, S. Chaugai, Q. Ning, C. Chen, D.W. Wang, Trimetazidine prevents macrophage-mediated septic myocardial dysfunction via activation of the histone deacetylase sirtuin 1, Br. J. Pharmacol. 173 (3) (2016 Feb) 545–561.
[6] S. Wang, K.S. Tan, H. Beng, F. Liu, J. Huang, Y. Kuai, R. Zhang, W. Tan, Protective effect of isosteviol sodium against LPS-induced multiple organ injury by regulating of glycerophospholipid metabolism and reducing macrophage-driven inflammation, Pharmacol. Res. 172 (2021 Oct) 105781.
[7] W. Cao, Y. Wang, X. Lv, X. Yu, X. Li, H. Li, Y. Wang, D. Lu, R. Qi, H. Wang, Rhynchophylline prevents cardiac dysfunction and improves survival in lipopolysaccharide-challenged mice via suppressing macrophage I-κBα phosphorylation, Int. Immunopharm. 14 (3) (2012 Nov) 243–251.
[8] F. Lu, Y. Hong, L. Liu, N. Wei, J. Lin, J. He, Y. Shao, Long noncoding RNAs: a potential target in sepsis-induced cellular disorder, Exp. Cell Res. 406 (2) (2021 Sep 15) 112756.
[9] W. Xie, L. Chen, L. Chen, Q. Kou, Silencing of long non-coding RNA MALAT1 suppresses inflammation in septic mice: role of microRNA-23a in the down-regulation of MCEMP1 expression, Inflamm. Res. 69 (2) (2020 Feb) 179–190.
[10] H. Jiang, J. Ni, Y. Zheng, Y. Xu, Knockdown of lncRNA SNHG14 alleviates LPS-induced inflammation and apoptosis of PC12 cells by regulating miR-181b-5p, Exp. Ther. Med. 21 (5) (2021 May) 497.
[11] Y. Zhu, Y. Wang, S. Xing, J. Xiong, Blocking SNHG14 antagonizes lipopolysaccharides-induced acute lung injury via SNHG14/miR-124-3p Axis, J. Surg. Res. 263 (2021 Jul) 140–150.
[12] S.M.K. Kingsley, B.V. Bhat, Role of microRNAs in sepsis, Inflamm. Res. 66 (7) (2017 Jul) 553–569.
[13] Y. Xu, C. Zhang, D. Cai, R. Zhu, Y. Cao, Exosomal miR-155-5p drives widespread macrophage M1 polarization in hypervirulent Klebsiella pneumoniae-induced acute lung injury via the MSK1/p38-MAPK axis, Cell. Mol. Biol. Lett. 28 (1) (2023 Nov 13) 92.
[14] H. Ouyang, Y. Tan, Q. Li, F. Xia, X. Xiao, S. Zheng, J. Lu, J. Zhong, Y. Hu, MicroRNA-208-5p regulates myocardial injury of sepsis mice via targeting SOCS2-mediated NF-κB/HIF-1α pathway, Int. Immunopharm. 81 (2020 Apr) 106204.
[15] Y. Cheng, J. Li, C. Wang, H. Yang, Y. Wang, T. Zhan, S. Guo, J. Liang, Y. Bai, J. Yu, G. Liu, Inhibition of long non-coding RNA metastasis-associated lung adenocarcinoma transcript 1 attenuates high glucose-induced cardiomyocyte apoptosis via regulation of miR-181a-5p, Exp. Anim. 69 (1) (2020 Jan 29) 34–44.
[16] Z. Huang, H. Xu, MicroRNA-181a-5p regulates inflammatory response of macrophages in sepsis, Open Med. 14 (2019 Nov 20) 899–908.
[17] S. Wang, Y. Zhang, HMGB1 in inflammation and cancer, J. Hematol. Oncol. 13 (1) (2020 Aug 24) 116.
[18] L. Pellegrini, E. Foglio, E. Pontemezzo, A. Germani, M.A. Russo, F. Limana, HMGB1 and repair: focus on the heart, Pharmacol. Ther. 196 (2019) 160–182.
[19] Y.N. Paudel, E. Angelopoulou, C. Piperi, V.R.M.T. Balasubramaniam, I. Othman, M.F. Shaikh, Enlightening the role of high mobility group box 1 (HMGB1) in inflammation: updates on receptor signalling, Eur. J. Pharmacol. 858 (2019) 172487.
[20] J. Yuan, L. Guo, J. Ma, et al., HMGB1 as an extracellular pro-inflammatory cytokine: implications for drug-induced organic damage, Cell Biol. Toxicol. 40 (1) (2024) 55.
[21] H. Yoo, Y. Im, R.E. Ko, J.Y. Lee, J. Park, K. Jeon, Association of plasma level of high-mobility group box-1 with necroptosis and sepsis outcomes, Sci. Rep. 11 (1) (2021) 9512.
[22] J. Pan, B. Alexan, D. Dennis, C. Bettina, L.I.M. Christoph, Y. Tang, microRNA-193-3p attenuates myocardial injury of mice with sepsis via STAT3/HMGB1 axis, J. Transl. Med. 19 (1) (2021) 386.
[23] R.K. Wolfson, E.T. Chiang, J.G. Garcia, HMGB1 induces human lung endothelial cell cytoskeletal rearrangement and barrier disruption, Microvasc. Res. 81 (2) (2011) 189–197.
[24] I. Popēna, A. Ābols, L. Saulīte, K. Pleiko, E. Zandberga, K. Jēkabsons, E. Endzeliņš, A. Llorente, A. Linē, U. Riekstiņa, Effect of colorectal cancer-derived extracellular vesicles on the immunophenotype and cytokine secretion profile of monocytes and macrophages, Cell Commun. Signal. 16 (1) (2018 Apr 24) 17.
[25] J. Chen, S. Tang, S. Ke, J.J. Cai, D. Osorio, A. Golovko, B. Morpurgo, S. Guo, Y. Sun, M. Winkle, G.A. Calin, Y. Tian, Ablation of long noncoding RNA MALAT1 activates antioxidant pathway and alleviates sepsis in mice, Redox Biol. 54 (2022 Aug) 102377.
[26] X. Long, X. Yao, Q. Jiang, Y. Yang, X. He, W. Tian, K. Zhao, H. Zhang, Astrocyte-derived exosomes enriched with miR-873a-5p inhibit neuroinflammation via microglia phenotype modulation after traumatic brain injury, J. Neuroinflammation 17 (1) (2020 Mar 19) 89.
[27] Y. Liu, L. Liu, J. Zhang, Protective role of matrine in sepsis-associated cardiac dysfunction through regulating the lncRNA PTENP1/miR-106b-5p axis, Biomed. Pharmacother. 134 (2021 Feb) 111112.
[28] H. Xu, W. Ye, B. Shi, LncRNA MALAT1 regulates USP22 expression through EZH2-mediated H3K27me3 modification to accentuate sepsis-induced myocardial dysfunction, Cardiovasc. Toxicol. 22 (9) (2022 Sep) 813–830.
[29] X. Lv, H. Wang, Pathophysiology of sepsis-induced myocardial dysfunction, Mil Med Res 3 (2016 Sep 27) 30.
[30] Y. Lin, Y. Xu, Z. Zhang, Sepsis-induced myocardial dysfunction (SIMD): the pathophysiological mechanisms and therapeutic strategies targeting mitochondria, Inflammation 43 (4) (2020 Aug) 1184–1200.
[31] K. Essandoh, Y. Li, J. Huo, G.C. Fan, MiRNA-mediated macrophage polarization and its potential role in the regulation of inflammatory response, Shock 46 (2) (2016 Aug) 122–131.
[32] V. Kumar, Targeting macrophage immunometabolism: dawn in the darkness of sepsis, Int. Immunopharm. 58 (2018 May) 173–185.
[33] X. Wang, Y. Ding, R. Li, R. Zhang, X. Ge, R. Gao, M. Wang, Y. Huang, F. Zhang, B. Zhao, W. Liao, J. Du, N6-methyladenosine of Spi2a attenuates inflammation and sepsis-associated myocardial dysfunction in mice, Nat. Commun. 14 (1) (2023 Mar 2) 1185.
[34] X. Sun, Y. Liu, J. Wang, M. Zhang, M. Wang, Cardioprotection of M2 macrophages-derived exosomal microRNA-24-3p/Tnfsf10 axis against myocardial injury after sepsis, Mol. Immunol. 141 (2022 Jan) 309–317.
[35] Z. Wang, M. Liu, D. Ye, J. Ye, M. Wang, J. Liu, Y. Xu, J. Zhang, M. Zhao, Y. Feng, S. Xu, W. Pan, Z. Luo, D. Li, J. Wan, Il12a deletion aggravates sepsis-induced cardiac dysfunction by regulating macrophage polarization, Front. Pharmacol. 12 (2021 Jul 2) 632912.
[36] W. Liang, J. Li, C. Bai, Y. Chen, Y. Li, G. Huang, X. Wang, Interleukin-5 deletion promotes sepsis-induced M1 macrophage differentiation, deteriorates cardiac dysfunction, and exacerbates cardiac injury via the NF-κB p65 pathway in mice, Biofactors 46 (6) (2020 Nov) 1006–1017.
[37] S. Liu, W. Chong, Roles of LncRNAs in regulating mitochondrial dysfunction in septic cardiomyopathy, Front. Immunol. 12 (2021 Nov 24) 802085.
[38] Q. Wang, Y. Xie, Q. He, Y. Geng, J. Xu, LncRNA-Cox2 regulates macrophage polarization and inflammatory response through the CREB-C/EBPβ signaling pathway in septic mice, Int. Immunopharm. 101 (Pt B) (2021 Dec) 108347.
[39] Y.Y. Luo, Z.Q. Yang, X.F. Lin, F.L. Zhao, H.T. Tu, L.J. Wang, M.Y. Wen, S.X. Xian, Knockdown of lncRNA PVT1 attenuated macrophage M1 polarization and relieved sepsis induced myocardial injury via miR-29a/HMGB1 axis, Cytokine 143 (2021 Jul) 155509.

[40] R. Zhang, Z. Niu, J. Liu, X. Dang, H. Feng, J. Sun, L. Pan, Z. Peng, LncRNA SNHG1 promotes sepsis-induced myocardial injury by inhibiting Bcl-2 expression via DNMT1, J. Cell Mol. Med. 26 (13) (2022 Jul) 3648–3658.

[41] M. Wang, J. Wei, F. Shang, K. Zang, P. Zhang, Down-regulation of lncRNA SNHG5 relieves sepsis-induced acute kidney injury by regulating the miR-374a-3p/TLR4/NF-κB pathway, J. Biochem. 169 (5) (2021 Jul 3) 575–583.

[42] N. Yang, H. Wang, L. Zhang, J. Lv, Z. Niu, J. Liu, Z. Zhang, Long non-coding RNA SNHG14 aggravates LPS-induced acute kidney injury through regulating miR-495-3p/HIPK1, Acta Biochim. Biophys. Sin. 53 (6) (2021 May 21) 719–728.

[43] H. Dong, C. Yang, X. Chen, H. Sun, X. He, W. Wang, Breast cancer-derived exosomal lncRNA SNHG14 induces normal fibroblast activation to cancer-associated fibroblasts via the EBF1/FAM171A1 axis, Breast Cancer 30 (6) (2023 Nov) 1028–1040.

[44] S. Luo, X. Huang, S. Liu, L. Zhang, X. Cai, B. Chen, Long non-coding RNA small nucleolar RNA host gene 1 alleviates sepsis-associated myocardial injury by modulating the miR-181a-5p/XIAP Axis in vitro, Ann. Clin. Lab. Sci. 51 (2) (2021 Mar) 231–240. PMID: 33941563.

[45] Y. Wang, Z. Xu, D. Yue, Z. Zeng, W. Yuan, K. Xu, Linkage of lncRNA CRNDE sponging miR-181a-5p with aggravated inflammation underlying sepsis, Innate Immun. 26 (2) (2020 Feb) 152–161.

[46] C. Deng, L. Zhao, Z. Yang, J.J. Shang, C.Y. Wang, M.Z. Shen, S. Jiang, T. Li, W.C. Di, Y. Chen, H. Li, Y.D. Cheng, Y. Yang, Targeting HMGB1 for the treatment of sepsis and sepsis-induced organ injury, Acta Pharmacol. Sin. 43 (3) (2022 Mar) 520–528.

[47] Y. Cheng, D. Wang, B. Wang, H. Li, J. Xiong, S. Xu, et al., HMGB1 translocation and release mediate cigarette smoke-induced pulmonary inflammation in mice through a TLR4/MyD88-dependent signaling pathway, Mol. Biol. Cell 28 (2017) 201–209.

[48] Z. Wang, W. Chen, Y. Li, S. Zhang, H. Lou, X. Lu, X. Fan, Reduning injection and its effective constituent luteoloside protect against sepsis partly via inhibition of HMGB1/TLR4/NF-κB/MAPKs signaling pathways, J. Ethnopharmacol. 270 (2021 Apr 24) 113783.

[49] S. Zheng, Y. Pan, C. Wang, Y. Liu, M. Shi, G. Ding, HMGB1 turns renal tubular epithelial cells into inflammatory promoters by interacting with TLR4 during sepsis, J. Interferon Cytokine Res. 36 (1) (2016 Jan) 9–19.